NORSAR

NORSAR Scientific Report No. 1-2004

Semiannual Technical Summary

1 July - 31 December 2003

Frode Ringdal (ed.)

Kjeller, February 2004

6.2 Source depths at regional distances: an example from the Western Barents Sea / Svalbard Region

6.2.1 Introduction

On 4 July 2003 at 07:16 an earthquake with a magnitude of mb 5.7 and Ms 5.1 (NEIC) occurred in the Flinn-Engdahl-Region Western Barents Sea, close to Hopen Island (see Figs. 6.2.1 and 6.2.2), which belongs to the Svalbard Archipelago (Norway). The analyst reviewed onset readings and an estimated hypocenter (event number 5487) are published on the web-page of the Norwegian National Data Center at NORSAR. An inspection of seismograms recorded at the stations and arrays (Fig. 6.2.1) collected at NORSAR revealed indications for a hypocenter within the crust, for instance due to the clear development of Lg waves.

The depth of the Mohorovicic discontinuity (Moho) in the Svalbard platform area is about 32 km (Faleide, 2000). Moho depths at the recording sites in Fennoscandia reach down below 40 km or even below 50 km beneath Finland. The 1D velocity model for routine analysis at NORSAR has a Moho depth of 41 km. The source depth of the event under consideration was determined to 45 km by the routine location procedure, hence, below the Moho.

The aim of this study was to relocate the event using classical and non-linear/probabilistic location procedures and to determine the reliability of the source depth determination. Because of the more principal character of this study the analyst reviewed onset parameters were used unchanged and no extra data were collected from additional stations, which may also have observed this event.

6.2.2 Classical location procedure

The results of the routine processing at NORSAR can be found in the bulletin of the Norwegian National Data Center (http://www.norsar.no/NDC/bulletins/regional/2003/07/5487.html). Seismogram records range from the Spitsbergen array at a distance of around 270 km to the Hagfors array at a distance of more than 1800 km. Located at 76.25˚ N and 22.75˚ E the epicenter uncertainty was given as an error ellipse with a major half axis of 50 km (strike 70˚) and a minor half axis of 12 km (see the blue solution in Fig. 6.2.2). A hypocentral depth error is not given by the routine analysis programme package. The solution given in the bulletin of the NEIC (weekly listings) moves the event 19 km to the north-east to an epicenter at 76.37˚ N and 23.28˚ E with a fixed depth of 10 km.

A relocation of the event was performed with the linearized inversion program HYPOSAT (Schweitzer, 2001), introducing a-priori time errors for P-picks of 1 s and for S-picks of 1.7 s. As shown by Hicks *et al.* (2004), the velocity model BAREY (Schweitzer & Kennett, 2002) is more appropriate for locating seismic events in the Barents Sea than the Fennoscandia model used in the routine analysi. Therefore, this model was used throughout this study to relocate the event. The resulting error ellipse (90-percent confidence level) was nearly circular with half axes of 12 km (strike 31˚) and 11 km, respectively (see the green solution in Fig. 6.2.2). Compared to the routine location the epicenter shifted towards North East and the new estimated source depth was calculated to 33 ±13 km.

6.2.3 Event location with the neighbourhood algorithm (NA)

The neighbourhood algorithm (Sambridge, 1999a; b) was applied for the inversion and confidence estimate of the location procedure. Localization with NA has already been implemented for instance by Sambridge & Kennett (2001) and the good convergence has been shown. The basic idea is a clever search of the parameter space invoking Voronoi cells and some measure of misfit, for instance X^2 (Chi squared, *e.g.*, Press *et al.*, 1986). This places the NA in a non-linear context comparable to genetic algorithms, simulated annealing and others. An important feature of the NA-sampler is its agility and the possibility to steer the convergence towards a misfit minimum by controlling the balance between exploration and exploitation of the parameter space. If convergence is achieved the solution of the non-linear location search is found as hypocenter coordinates (see also Schweitzer & Kennett, 2002).

In a second step, the sampling of the parameter space is used to compute a Bayesian estimate of the posterior probability-density distribution (PPD) of the location result (Sambridge, 1999b). In the case described here, the parameter space has three dimensions: latitude, longitude and depth of the hypocenter. The source time was found to converge to a stable value in the sampling process when the mean time residual of all phase readings was forced to vanish. Hence, the source time was not introduced as a free parameter of its own.

The initially sampled subregion of the parameter space, ranged 100 km in each coordinate direction. The convergence of the iteration process to a solution was very fast and reached the hypocenter marked in red in Figs. 6.2.2 and 6.2.3.

To illustrate and evaluate the complete (3-dimensional) PPD, 2D-marginals were computed (Sambridge, 1999b). These marginals are projections of the PPD onto two dimensions, for instance longitude-latitude or latitude-depth, from which confidence levels can be calculated. In Fig. 6.2.2 the contour of the 90-percent confidence level of the longitude-latitude marginal is directly comparable to the 90-percent error ellipses of the classical location procedures. Finally, the maximum of the 2D-marginal - that is the region of highest probability - can be compared to the result of the non-linear search. With only three free parameters the discrepancy of the epicenter in the presented example was found to be very small (Fig. 6.2.2). Other than the HYPOSAT result, the 90-percent confidence region shows an elongation similar to that of the routine error ellipse without reaching its size. Explanations for these discrepancies remain yet speculative.

Schweitzer & Kennett (2002) compared the classical and the NA location procedure in case of an event in the Kara Sea and found a satisfying consistency of the epicenters. On the other hand, the strong influence of applying the “right” Earth model became evident.

Another probabilistic approach (Lomax & Curtis, 2001) was utilized by Husen *et al.* (2003) to evaluate structure and hypocenters in Switzerland.

6.2.4 Source depth estimates

Fig. 6.2.3 comprises the available source depth estimates for the event in a vertical section with view from the East (latitude versus depth). The routine analysis depth of 45 km is depicted as a blue dot, the HYPOSAT determination is shown in green at 33 km with its 13 km-error bar, and the NA estimated depth is shown as a red dot. The 2D-marginal from the NA-procedure is shaded in gray with the 90-percent confidence contour depicted. The 90-percent region reaches from 20 to 60 km depth. Below the Moho the probability density broadens in latitude. The probability for the hypocenter to be situated above or below the Moho is nearly even. In classical terms an uncertainty of more than 20 km should be assigned to the source depth.

At smaller epicentral distances as well as for teleseismic events additional information can be used to improve source depth estimates. Reflections from the Moho (PmP, SmS) or depth phases (pP, sP) provide useful constraints. Unfortunately, at regional distances, only full waveform inversion could improve the generally poor depth resolution, but only if the velocity model is really well known. Here we can only use the appearance of strong Lg waves as indication for a crustal event, which will make both hypocenter estimates (NA and HYPOSAT) more similar.

6.2.5 Earth model variations

The NA was used to evaluate the influence of our deficient knowledge of the Earth – that is the uncertainties in the velocity structure – on the error estimation of hypocenter determinations. The principles of the NA are not effected by the degrees of freedom, although the sampling and integration have to be performed in a higher-dimensional parameter space. Of course, it does not make sense to allow for model variations in regions where there is no resolution (*e.g.*, no ray-path coverage). This might only lead to instability when evaluating the Bayesian estimate of the PPD.

For the example studied here deviations of ±5 percent for P and S wave velocities in the crust were permitted for start model BAREY. Layer depths and mantle velocities were kept constant. Even with these relative moderate deviations, the resulting confidence region turned out to be huge (Fig. 6.2.4). The 90-percent contour of the latitude-depth marginal now comprises nearly the entire sampled parameter space-subregion ($100 \times 100\ km^2$). Essentially, the specification of a source depth became nearly meaningless. The only statement could read: probably not deeper than 100 km.

6.2.6 Conclusion

Classical event location procedures using travel times mainly underestimate the uncertainty of source-depth determinations, in particular, in such cases for which the azimuthal coverage of observations is very uneven or nearby observations are missing. More realistic error estimates are yielded by using techniques like the Bootstrap or Monte Carlo search. A complete picture can only be derived from a thoroughly computed PPD. For the presented example the confidence regions are at most in the same order of magnitude as the classical error bars or ellipses.

But, one of the most important unknowns for locating earthquakes is the velocity structure. Incorporating only a 5-percent uncertainty of the crustal velocities led to nearly meaningless source depth estimates. The 90-percent confidence region extends over more than a hundred kilometers in depth, which can only be restricted with further seismological evidence like the occurrence of Lg or Rg. However, it has to be concluded that this result throws a rather negative light on studies which use source depths from catalogues. Improvements are conceivable with good station coverage at short distances and an excellent knowledge of the velocity distribution within the Earth.

Acknowledgements

In 2003, a 2-month research term of StS at NORSAR was funded through the EC programme Access to Research Infrastructure-project (Contract HPRI-CT-2002-00189). Figures were plotted with GMT (Wessel & Smith, 1991).

Stefan Stange, Landeserdbebendienst Baden-Württemberg, Freiburg, Germany

Johannes Schweitzer

References

Faleide, J. I. (2000). Crustal structure of the Barents Sea – important constraints for regional seismic velocity and travel-time models. NORSAR Sci. Rep. **2-1999/2000**, 119-129.

Hicks, E. C., T. Kværna, S. Mykkeltveit, J. Schweitzer & F. Ringdal (2004). Travel-times and attenuation relations for regional phases in the Barents Sea region. Pure appl. Geophys. **161**, 1-19.

Husen, St., E. Kissling, N. Deichmann, St. Wiemer, D. Girardini & M. Baer (2003). Probabilistic earthquake location in complex three-dimensional velocity models: Application to Switzerland. J. Geophys. Res. **108(B2)**, 5, 1-20.

Lomax, A. & A. Curtis (2001). Fast, probabilistic earthquake location in 3D models using Oct-Tree Importance sampling. Geophys. Res. Abstr. **3**, 2001.

Press, W. H., B. P. Flannery, S. A. Teukolsky & W. T. Vetterling (1986). *Numerical Recipes*, Cambridge University Press, New York, 993 pp.

Sambridge, M. S. (1999a). Geophysical inversion with a neighbourhood algorithm – I. Searching the parameter space. Geophys. J. Int. **138**, 479-494.

Sambridge, M. S. (1999b). Geophysical inversion with a neighbourhood algorithm – II. Appraising the ensemble. Geophys. J. Int. **138**, 727-746.

Sambridge, M. S. & B. L. N. Kennett (2001). Seismic Event Location: Nonlinear Inversion Using a Neighbourhood Algorithm. Pure appl. Geophys. **158**, 241-257.

Schweitzer, J. (2001). HYPOSAT – An enhanced routine to locate seismic events. Pure appl. Geophys. **158**, 227-289.

Schweitzer, J. & B. L. N. Kennett (2002). Comparison of location procedures – The Kara Sea event of 16 August 1997. NORSAR Sci. Rep. **1-2002**, 97-114.

Wessel, P. & W. H. F. Smith (1991). Free software helps map and display data. EOS Trans. Amer. Geophys. U. **72(41)**, 441, 445-446.

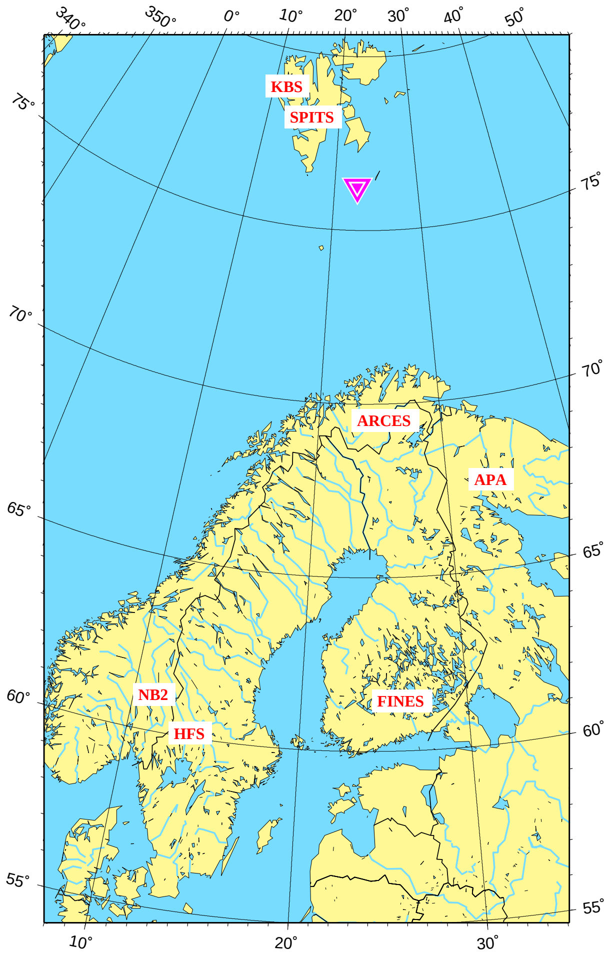

Fig. 6.2.1. *Map of the 4 July 2003 event (inverted triangle) with recording arrays and stations.*

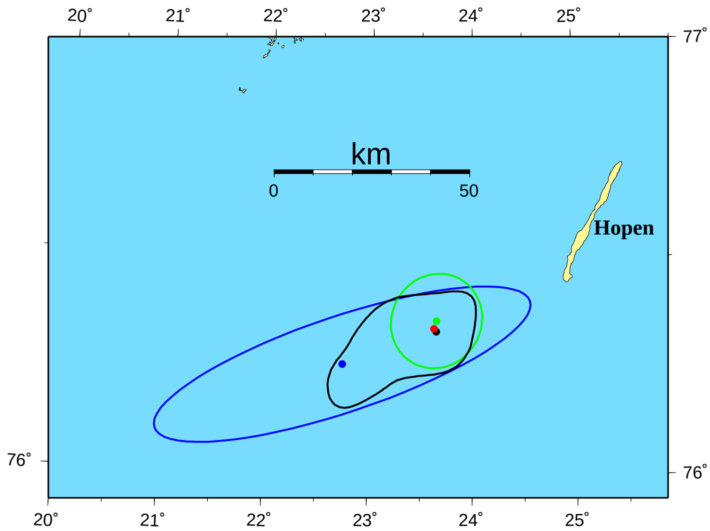

Fig. 6.2.2. *Epicenter map of the routine location (blue with error ellipse), the HYPOSAT location (green with error ellipse) and the NA location (red and black with 90-percent confidence region).*

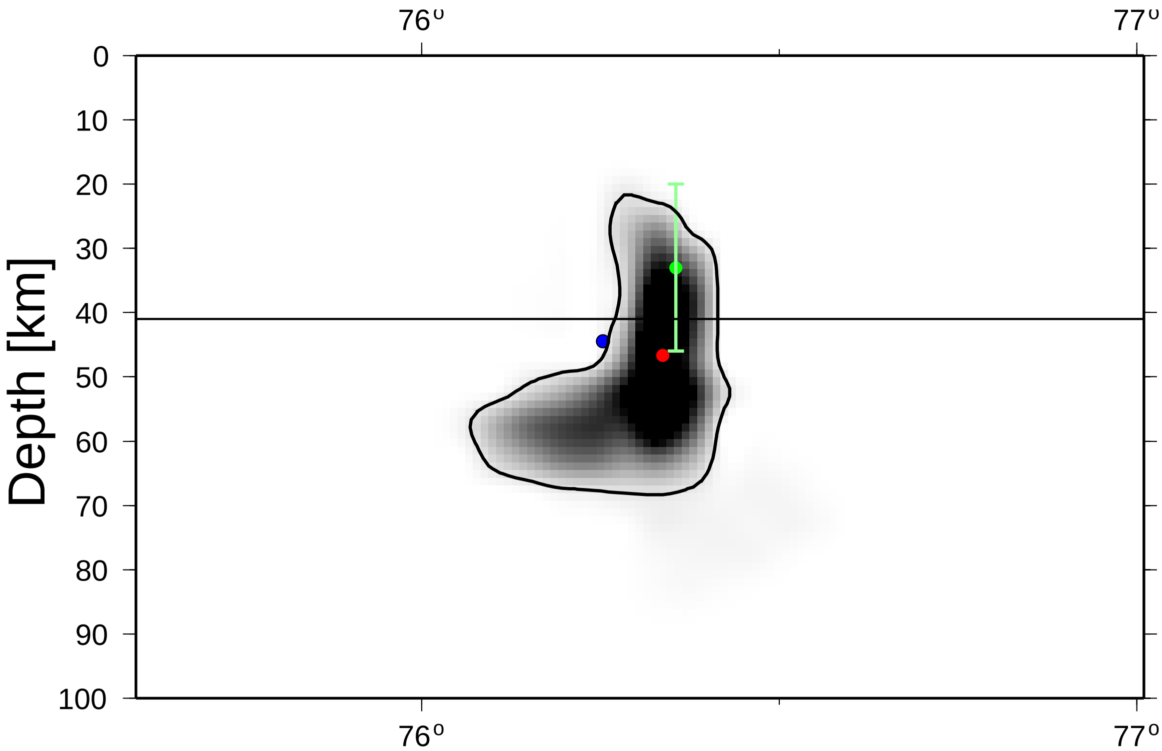

Fig. 6.2.3. *Latitude-depth section of the PPD-marginal (gray shading) and the 90-percent confidence contour. Green: HYPOSAT location with error bar. Blue: routine location. Red: NA location. The horizontal line indicates the Moho.*

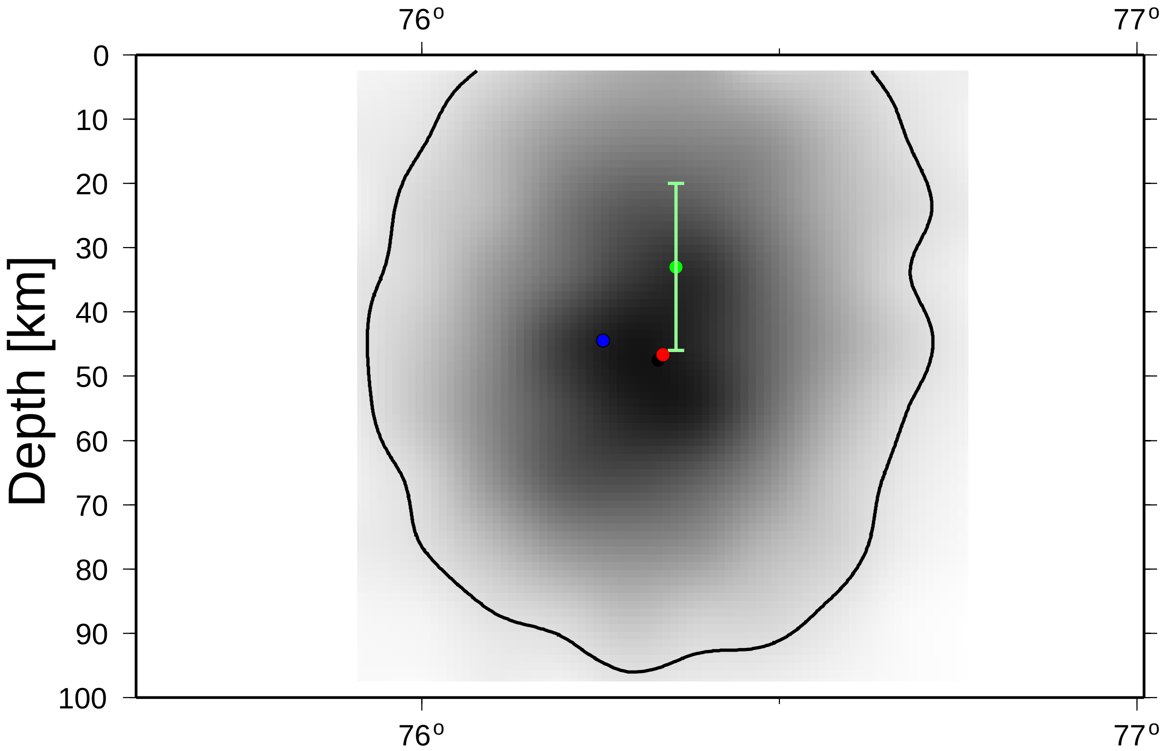

Fig. 6.2.4. *Same as Fig. 6.2.3 for the PPD-marginal computed including velocity model-variations.*